

Date of publication xxxx 00, 0000, date of current version xxxx 00, 0000.

Digital Object Identifier 10.1109/X.DOI

# Air Quality and Healthy Ageing: Predictive Modelling of Pollutants using CNN Quantum-LSTM

FAREENA NAZ<sup>1</sup>, MUHAMMAD FAHIM<sup>1</sup>, ADNAN AHMAD CHEEMA<sup>2</sup>, BRADLEY D. E. MCNIVEN<sup>6</sup>, TUAN-VU CAO<sup>4</sup>, RUTH HUNTER<sup>5</sup>, AND TRUNG Q. DUONG<sup>1,6</sup>, (FELLOW, IEEE)

<sup>1</sup>School of Electronics, Electrical Engineering and Computer Science, Queen's University Belfast, BT7 1NN, United Kingdom (e-mail: {fnaz01, m.fahim, trung.q.duong}@qub.ac.uk)

<sup>2</sup>School of Engineering, Ulster University, Belfast, BT15 1AP, United Kingdom (e-mail: a.cheema@ulster.ac.uk)

<sup>4</sup>Norwegian Institute for Air Research, Oslo, Norway (e-mail: tv@nilu.no)

<sup>5</sup>Centre for Public Health, School of Medicine, Dentistry and Biomedical Sciences, Queen's University Belfast, BT7 1NN, United Kingdom (e-mail: ruth.hunter@qub.ac.uk)

<sup>6</sup>Faculty of Engineering and Applied Science, Memorial University of Newfoundland, St. John's, NL A1C 5S7, Canada (e-mail: tduong@mun.ca)

Corresponding author: Trung Q. Duong (e-mails: trung.q.duong@qub.ac.uk).

The work of Muhammad Fahim, Tuan-Vu Cao was supported in part by UKRI and European Commission under MISO Project, "Autonomous Multi-Format In-Situ Observation Platform for Atmospheric Carbon Dioxide and Methane Monitoring in Permafrost and Wetlands." The work of Ruth Hunter was supported by the SPACE (Supportive Environments for Physical and Social Activity for Cognitive Health) Project (<https://www.qub.ac.uk/sites/space/>) funded by the ESRC Healthy Ageing Challenge under Grant ES/V016075/1. The work of T. Q. Duong was supported in part by the Canada Excellence Research Chair (CERC) Program CERC-2022-00109.

**ABSTRACT** The concept of healthy ageing is emerging and becoming a norm to achieve a high quality of life, reducing healthcare costs and promoting longevity. Rapid growth in global population and urbanisation requires substantial efforts to ensure healthy and supportive environments to improve the quality of life, closely aligned with the principles of healthy ageing. Access to fundamental resources which include quality healthcare services, clean air, green and blue spaces plays a pivotal role in achieving this goal. Air quality, in particular, is a critical factor in achieving healthy ageing targets. However, it necessitates a global effort to develop and implement policies aimed at reducing air pollution, which has severe implications for human health including cognitive impairment and neurodegenerative diseases, while promoting healthier environments such as high quality green and blue spaces for all age groups. Such actions inevitably depend on the current status of air pollution and better predictive models to mitigate the harmful impact of emissions on planetary health and public health. In this work, we proposed a hybrid model referred as AirVCQnet, which combines the variational mode decomposition (VMD) method with a convolutional neural network (CNN) and a quantum long short-term memory (QLSTM) network for the prediction of air pollutants. The performance of the proposed model is analysed on five key pollutants including fine Particulate Matter PM<sub>2.5</sub>, Nitrogen Dioxide (NO<sub>2</sub>), Ozone (O<sub>3</sub>), PM<sub>10</sub>, and Sulphur Dioxide (SO<sub>2</sub>), sourced from air quality monitoring station in Northern Ireland, UK. The effectiveness of the proposed model is evaluated by comparing its performance with its equivalent classical counterpart using root mean square error (RMSE), mean absolute error (MAE), and R-squared (R<sup>2</sup>). The results demonstrate the superiority of the proposed model, achieving a performance gain of up to 14% and validating its robustness, efficiency and reliability by leveraging the advantages of quantum computation.

**INDEX TERMS** Air pollution, CNN-QLSTM, healthy ageing, predictive models, quantum machine learning.

## I. INTRODUCTION

AIR pollution poses the greatest global environmental challenge of this era, directly impacting our planet and public health across the lifespan. Key air pollutants include fine Particulate Matter PM<sub>2.5</sub>, Nitrogen Dioxide

(NO<sub>2</sub>), Ozone (O<sub>3</sub>), PM<sub>10</sub>, and Sulphur Dioxide (SO<sub>2</sub>) are emitted into the air from fossil fuel combustion, transportation and various non-exhaust industrial emissions [1]. Recent research indicates extensive strong evidence of serious

health implications on individuals' health when exposed to environments that exceed World Health Organisation (WHO) recommended air quality standards, contributing to around 6.7 million premature deaths globally each year [2], [3]. The United Nations (UN) established sustainable development goals (SDGs), specifically 3, 7 and 11 reflect the urgency to reduce morbidity, mortality, and adverse environmental effects through specific targets to advance public health, directly contributing to the broader realm of the healthy ageing, and promote sustainable urban growth [4]. However, the United Kingdom (UK) government aims to achieve a 35% reduction in air pollution by 2030 [5]. Even with growing global awareness and policies, research on the impact of air pollution on vulnerable and elderly groups needs further exploration to better understand, manage and model air pollution for a better tomorrow's digital world aligned with UK Clean Air Strategy roadmap and 25 Year Environment Plan (25YEP) [6], [7].

The global population is ageing, and medical advancements are helping people live longer. However, achieving longevity with healthy ageing is crucial. By 2050, the population aged 60 years or over is expected to double, with a significant proportion expected to live in urban areas [8]. The swift growth in urbanisation along with demographic shift, necessitates ecological upgrades to ensure a healthier environment that supports healthy ageing for a growing population. To achieve this, reduction in air pollution is vital, as exposure to pollutants causes serious health implications such as respiratory, cardiovascular, and chronic lung diseases. Cohort studies show a positive correlation between PM<sub>2.5</sub> exposure and the elevated risk of cognitive decline and dementia [9]–[12]. Another high risked pollutant, NO<sub>2</sub> is also explored and is being associated with a high risk of dementia, Parkinson's, and Alzheimer disease [11], [13]–[15]. For instance, Japan has an ageing population with 30% of the people already aged 60 years or over and is the only Asian country working towards a net zero transition while considering the challenges related to its ageing society. Similarly, China has also acknowledged the need to adapt to and mitigate climatic changes to protect vulnerable elderly populations from health risks associated with extremes of heat.

The UN has declared 2021–2030 as the "Decade of Healthy Ageing", led by the WHO. This global collaboration is a united effort to help people live healthy longer lives over the next decade [8]. The primary objective is to improve the elderly population's lives by building supportive environments and providing access to personalised care. To address and support the challenges of healthy ageing, the UK government invested in research and innovation (via UKRI) by allocating a budget of £98 million in different projects including our SPACE (Supportive Environments for Physical and Social Activity, Healthy Ageing, and Cognitive Health) project [16]. In this work, as part of SPACE project, we are exploring better models for air pollution prediction which can be further used to overcome the challenges of

healthy ageing and urban environments. Promoting healthier urban environments is crucial not only to mitigate widespread health risks and to improve the quality of life for the ageing population but also to address climate challenges, support net zero emissions and ensure sustainable living for all. This demands a substantial reduction in air pollution, hotspot identifications and accurate air pollution prediction. The primary objective of this work is to develop air pollution prediction models using emerging concepts of quantum machine learning. We anticipate that findings from this work will provide evidence-based insight and lead to developing policies and programmes that improve the urban environment for healthy ageing, life expectancy and quality of life for everyone. The main contributions of this work include:

- We proposed a hybrid forecasting model i.e. AirVCQnet using a combination of variational mode decomposition (VMD) to generate frequency dependent features, which are further used to extract complex features using convolutional neural network (CNN). Such features are further used by quantum long short-term memory (QLSTM) models to capture time dependencies for an improved prediction. To the best of our knowledge, this is the first time quantum machine learning is used to predict air pollutants in the realm of healthy ageing and climate change.
- We have performed a detailed experimental investigation to find the optimum parameters of VMD, CNN, four qubit variational quantum circuit (VQC) and QLSTM to obtain improved performance based on real-world dataset, local to Northern Ireland, for five pollutants including fine PM<sub>2.5</sub>, NO<sub>2</sub>, O<sub>3</sub>, PM<sub>10</sub>, and SO<sub>2</sub>.
- We have proposed five bespoke forecasting models having similar model architecture with a unique set of hyperparameters for each of the five respective pollutants. We have evaluated the performance of the proposed models using root mean square error (RMSE), mean absolute error (MAE), and R-squared (R<sup>2</sup>) and provided a comparison to the equivalent classical model (i.e., VMD-CNN-LSTM having same architecture and hyperparameters) for each pollutant. To the best of our knowledge, this is the first study which provides a head-to-head comparison of a benchmark quantum based model to its classical counterpart with same architecture and parameters on the air pollution data.

The rest of the paper is organised as follows: related work is provided in Section II. Fundamentals of quantum computing are explained in Section III. Section IV describes the dataset and Section V provides technical details of the proposed model. Model training and testing are discussed in Section VI. Results and discussion is presented in Section VII. Lastly, the findings are concluded in Section VIII.

## II. RELATED WORK

Air quality and healthy ageing represents two sides of the same coin, as poor air quality exacerbates age related health issues. However, accurate pollution prediction to address

potential health and climate challenges is necessary. Recent technological advancement by leveraging machine learning through hybrid and ensemble modelling has made significant progress in air pollution prediction. However, recently quantum machine learning has gained considerable attention and has been extensively explored for its potential in time series prediction.

A recent study proposed a temporal change information learning method for dynamic sequence modelling, where a variant of long short-term memory (LSTM) namely transformation LSTM is proposed to capture rapid and slow changes in information (historical data) [17]. Additionally, the study also proposed a new objective function and optimisation algorithm named adaptive moment estimation forgetting gradient to attain effective optimal parameters for modelling multivariate time series data. To check the effectiveness of the proposed model, a comprehensive analysis is performed using three different datasets (i.e. weather, PM2.5 air quality, and energy consumption dataset), and the results show the superiority of the proposed method over others based on evaluation metric MAE and RMSE. A unified machine learning architecture for air pollutants prediction is proposed in [18]. The proposed architecture is based on lightGBM and RF regressor to capture spatiotemporal dependencies in data. Six months' data collected from distinct locations including Malaysia, India and the Philippines is used to train the model, taking into consideration all relevant direct and indirect factors dependencies on target pollutants to predict the following day. The proposed approach performed well in comparison to a recurrent neural network (RNN) and transformer models in terms of RMSE. In [19], a study made comparison of two hybrid models namely CNN-LSTM and CONV-LSTM with combinational differences of CNN and LSTM layers in its architecture. The dataset used consists of 1488 data samples, recorded on an hourly resolution to predict PM2.5 concentration for the next few hours in Kemayoran district of Central Jakarta, Indonesia. Findings revealed the performance of CONV-LSTM better than other over assessment indicators like RMSE, MAE and MAPE.

A hybrid deep learning model is proposed by combining bidirectional LSTM (BiLSTM), bidirectional gated recurrent unit (BiGRU) and fully connected layers [20]. Where the BiLSTM and BiGRU layer extract initial and deep features respectively, which are further used by fully connected layers to predict hourly PM2.5 concentration at multiple locations in China. The dataset contains 35064 hrs of data from each monitoring station including 12 air pollutants and numerous meteorological factors to capture intricate relationships between data. In [21], proposed another hybrid approach for short-term prediction of PM2.5 concentrations by incorporating wavelet denoising, VMD and principal component analysis for the feature extraction and BiLSTM neural network for modelling data. The experimental data is comprised of 30198 hrs including various air pollutants and meteorological factors and is collected from Quzhou city, Zhejiang Province. The proposed model used previous 24 hr multivariate data

to predict the following hour. Findings from experiments validated the efficacy of the proposed model. A multivariate time series prediction model is proposed using Beijing AQI dataset comprised of 4320 data samples [22]. The study modified the binary salp swarm algorithm for the selection of features and parameters optimisation simultaneously. The echo state network (ESN) model is employed for PM2.5 concentration prediction by incorporating seven air pollutant data as input features. Results show the effectiveness of the MBSSA-ESN model over BSSA-ESN and other models optimised by evolutionary algorithms using standard indicators. The study in [23] proposed a lightweight GRU model and employed the spatial temporal correlation of multi-node data to improve the prediction accuracy of air quality forecasting. The effectiveness of the approach is validated using a publicly available Intel lab dataset and attained reduced error scores in terms of RMSE and MAE in comparison to single node based prediction. In [24], the combination of GRU and graph convolution network is proposed for the prediction tasks like traffic and air quality prediction across cities. The study proposed a spatiotemporal prediction model with transfer knowledge to solve data scarcity issues. Experimental analysis is conducted using datasets collected from London and Beijing, and the results indicate that the proposed domain adversarial model outperformed other models.

In recent years, quantum computing has gathered much attention because of its higher computational advantages over classical computing. Machine learning algorithms using quantum computing, also known as quantum machine learning, are rapidly growing, and catching researchers' interest towards its potential application in numerous fields such as renewable energy, intelligent transportation systems, natural language processing, finance, and wireless communication [25]–[29]. Recent research shows the superiority of quantum machine learning over classical machine learning where quantum computing is exploited to improve machine learning algorithms with the initial thought of accelerating the training process in potential applications [30]. A hybrid quantum LSTM network is proposed by embedding VQC in LSTM to improve the solar irradiance prediction accuracy [31]. The considered dataset is comprised of four years and is collected from five cities in China. Solar irradiance and meteorological data (such as wind speed, press, solar zenith angle, humidity, temperature, dew point, cloud and GHI) of the previous 24 hrs is used for the hour ahead prediction. The results are evaluated using standard evaluation metrics RMSE, MAE and  $R^2$  score and compared with other models (SARIMA, CNN, RNN, GRU and LSTM). In a similar study [32], a hybrid classical quantum model is proposed, which combines the classic LSTM model with a quantum neural network (QNN) for wind speed forecasting. The proposed model used 2D wind speed data of the previous 32 hrs to forecast the wind speed of the farm situated in Fuhai, Taiwan for the following 24 hrs. The used dataset is collected from seven locations across various countries, spanning a year. For hyperparameter selection, Taguchi orthogonal experiments were

performed. The study used QNN with 10 qubit system and the quantum circuits with a depth of 2 repetitions showed the best score. The proposed approach outperformed five other models (RF, SVR, XGBoost, NAR, LSTM Autoencoder, and LSTM) and is evaluated using performance indicators such as RMSE, MAE and  $R^2$  score.

Quantum computing is utilised by integrating quantum inspired neural network model with deep learning model. Where the quantum inspired neural network and LSTM replace the fully connected layer of CNN to enhance the prediction accuracy of wind speed [33]. Additionally, quantum particle swarm optimisation is employed for optimising the parameters of the model architecture. The 2D spatiotemporal dataset is collected from four different locations to predict the wind speed of the following day of Fuhai, Taiwan. The dataset used is of one year with an hourly wind speed resolution. The comprehensive analysis with other models (XGBoost, DBM, ARIMA-ANN, GRNN, LSTM-M, CNN-LSTM, CNN-LSTM-FC, CNN-LSTM-CVNN) demonstrates the effectiveness of the proposed model and is validated using evaluation indicators RMSE, MAE and  $R^2$ . In [34], a hybrid quantum classical recurrent neural network (QRNN) is proposed for the prediction of renewable energy of time series data. The photovoltaic output power data is comprised of one year and is collected from a power production plant situated in Oak Ridge, TN, USA. The model is composed of two cascaded classical LSTM layers with a fully connected layer and is integrated with a variational quantum (VQ) layer. To exploit the entanglement and superposition properties of quantum, the considered VQ layer consists of a 2 qubit system, ZZFeatureMap with linear entanglement and depth 2. To process the information, RealAmplitude ansatz circuit with depth 1 and linear entanglement is considered followed by the measurement layer to produce the expected outcome based on the Pauli-Z gate. The study conducted an experimental analysis of four seasons and compared the performance of the proposed model with the LSTM and RF model using RMSE as an assessment indicator and showed better results in terms of reduced error score as compared to the classical counterparts. A linear-layer-enhanced quantum LSTM (LQLSTM) model is proposed based on QLSTM for carbon price forecasting [35]. The study introduced a shared linear embedding layer before VQC, which by compressing the input features subsequently reduces the number of qubits and improves learning. However, a separate linear embedding layer is preferred after VQCs to get different information according to each VQC's functionality. Additionally, a strongly entangled controlled-Z gate is preferred over CNOT gate in the variation layer. The dataset is comprised of four years and is collected from European Union Emission Trading. Comprehensive analysis shows the performance of LQLSTM model is better than QLSTM in terms of reduced RMSE and MAE value but comparable to LSTM.

### III. QUANTUM COMPUTING FUNDAMENTALS

In this section, we provided an overview of the fundamentals of quantum computing to contextualise the methods and models employed in this work. Quantum information is represented by a qubit and is defined by its quantum state  $|\psi\rangle$  as

$$|\psi\rangle = p_0|0\rangle + p_1|1\rangle, \quad (1)$$

where  $p_0$  and  $p_1$  are the probability amplitudes which satisfy  $|p_0|^2 + |p_1|^2 = 1$ .

In this work, we have used a combination of quantum gates in our VQC which we define below in detail.

- **Hadamard Gate ( $H$ )** is used to create a superposition between qubits and is defined as

$$H = \frac{1}{\sqrt{2}} \begin{pmatrix} 1 & 1 \\ 1 & -1 \end{pmatrix}. \quad (2)$$

- **Rotation Gates ( $R_x, R_y, R_z$ )** are used to rotate a given qubit state around the  $x$ ,  $y$ , and  $z$  axes of the Bloch sphere, respectively. These operations change a qubit's position on the Bloch sphere based on the rotation angle  $\theta$ . The three rotation gates are defined as:

$$R_x(\theta) = \begin{pmatrix} \cos(\frac{\theta}{2}) & -i \sin(\frac{\theta}{2}) \\ -i \sin(\frac{\theta}{2}) & \cos(\frac{\theta}{2}) \end{pmatrix}, \quad (3)$$

$$R_y(\theta) = \begin{pmatrix} \cos(\frac{\theta}{2}) & -\sin(\frac{\theta}{2}) \\ \sin(\frac{\theta}{2}) & \cos(\frac{\theta}{2}) \end{pmatrix}, \quad (4)$$

$$R_z(\theta) = \begin{pmatrix} e^{-i\theta/2} & 0 \\ 0 & e^{i\theta/2} \end{pmatrix}. \quad (5)$$

- **Controlled-NOT Gate (CNOT)** provides one of the essential operations in quantum processing by entangling quantum states. As defined in eq. 6, the 2-qubit CNOT operation flips the state of the target qubit if the control qubit is in state  $|1\rangle$ , otherwise the state remains unchanged.

$$\text{CNOT} = \begin{pmatrix} 1 & 0 & 0 & 0 \\ 0 & 1 & 0 & 0 \\ 0 & 0 & 0 & 1 \\ 0 & 0 & 1 & 0 \end{pmatrix}. \quad (6)$$

- **Pauli-Z Gate ( $P_z$ )** is commonly used in the measurement stage where it performs a phase flip of state  $|1\rangle$ , leaving the state  $|0\rangle$  unchanged.  $P_z$  is defined as:

$$P_z = \begin{pmatrix} 1 & 0 \\ 0 & -1 \end{pmatrix}, \quad (7)$$

and when applying  $P_z$  to eq. 1, one obtains  $P_z|\psi\rangle = p_0|0\rangle - p_1|1\rangle$ , which has eigenvalues of  $+1$  and  $-1$  which correspond to the states  $|0\rangle$  and  $|1\rangle$ , respectively.

#### IV. DATASET

In this study, the experiments are conducted using a publicly available dataset collected from Air Quality Northern Ireland, UK [36]. The dataset contains air quality parameters, which include the key air pollutants such as PM<sub>2.5</sub>, NO<sub>2</sub>, O<sub>3</sub>, PM<sub>10</sub> and SO<sub>2</sub>. The dataset contains hourly concentration levels of the aforementioned pollutants and is comprised of 1440 hrs used for experimental analysis. The descriptive statistical information of the air quality parameters is provided in Table. 1. This provides insight into total count, mean, and standard deviation along with their respective minimum and maximum values for all major pollutants. The mean and standard deviation range between 1.78 to 38.60 and 1.94 to 21.21, respectively. Additionally, the minimum and maximum values fall between 0 to 1 and 19 to 129 for all the pollutants. The dataset is pre-processed to remove outliers and invalid values using interquartile range (IQR) method.

TABLE 1. Statistics of key air pollutants in  $\mu\text{g}/\text{m}^3$ .

	Count	Mean	Std	Min	25%	50%	75%	Max
PM <sub>2.5</sub>	1440	11.26	10.11	0	6	8	12.76	84
NO <sub>2</sub>	1440	32.24	20.78	1	15	29.42	44.50	129
O <sub>3</sub>	1440	38.60	21.21	1	21	40	56	94
PM <sub>10</sub>	1440	16.58	11.78	0	9	13	20	97
SO <sub>2</sub>	1440	1.78	1.94	0	1	1	2	19

#### V. PROPOSED MODEL

In this section, we provide a background of our proposed model AirVCQnet which is a combination of VMD approach and CNN (aka ConvID) layers to generate new features, a Max-Pooling layer for down-sampling and a QLSTM layer for time series forecasting. Fig. 1 provides the architecture of the proposed model network architecture.

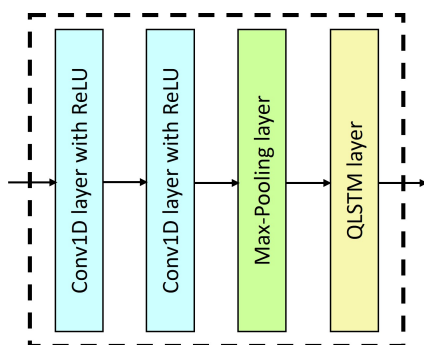


FIGURE 1. Proposed model network architecture.

##### A. VMD

VMD is a signal processing approach which decomposes a signal into a finite number of signals (also refer as sub-series or IMFs) by exploiting spectral properties [37]. Each IMF, bandlimited in nature, is defined by a unique spectral component and can capture frequency dependant unique

trends which can be useful in time series forecasting challenges [38]. Considering a time series  $V(t)$ , the series can be decomposed into  $K$  IMFs using:

$$v_k(t) = B_k(t)\cos(\phi_k(t)), \quad (8)$$

$$V(t) = \sum_{k=1}^K v_k(t) + R, \quad (9)$$

where  $v_k(t)$  is a  $k^{\text{th}}$  IMF with a amplitude of  $B_k(t)$  and phase of  $\phi_k(t)$ . Here,  $R$  refers to as residual signal and a unique spectral component of each IMF can be found using a derivative of the  $\phi_k(t)$ . In this work, we are using VMD approach to create new features using the hourly lag of the respective pollutant time series. Fig. 2 shows the VMD decomposition of the hourly lag of the PM<sub>2.5</sub> pollutant with  $K = 5$  where each IMF captures different trends. In the case of the VMD based features for time series forecasting challenges, it is of utmost importance to select an optimum value of the  $K$  with the intention to improve the prediction performance metrics. We have performed several trials to find the best value of the  $K$  with the objective to enhance the performance of the forecasting model.

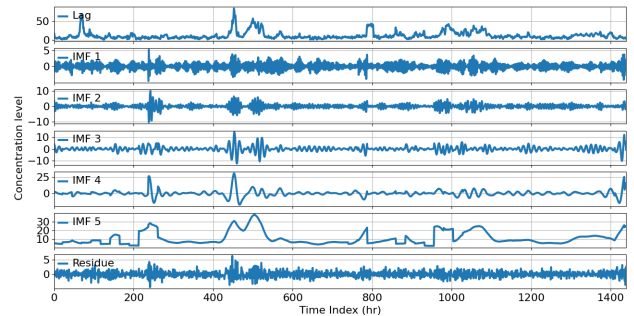


FIGURE 2. Decomposition of lag PM<sub>2.5</sub> into IMFs and Residual plot.

##### B. CNN

In recent years, CNN has become a popular approach to generate new features, also refer as feature map, in various fields for forecasting and classification problems [39], [40]. In a nutshell, a CNN layer uses a filter or kernel with weights and calculates a dot product between the weights and data of the time series to produce a new sample. By doing so, samples of the new feature can be extracted by sliding the filter over the given time series. The CNN's ability to capture local patterns depends on the kernel size which is referred to as the length of the filter and requires careful selection. In addition to this, various filters different in their weights can be used to generate multiple new features and number of output features by a CNN layer is defined by out channel parameter. We are using ReLU activation function on the newly generated features for each CNN layer to introduce nonlinearity. In our proposed model, we are using two CNN

layers and tuning the kernel size and out channel parameters to improve the performance of the prediction. Followed by CNN layers, we are using a Max-Pooling layer to reduce the newly generated information.

### C. QLSTM

The LSTM network is a variant of the RNN, specifically developed to mitigate the vanishing gradient problem faced by traditional RNNs [41]. This is what makes LSTM much more effective in significantly improving the performance over tasks such as time series forecasting, natural language processing, and speech recognition, where capturing long-term dependencies is crucial. LSTM achieved this by introducing the cell state and gates, where the cell state acts as long-term memory capable of selectively retaining and forgetting information over time and the flow of information is controlled by gates. Fig. 3 presents a functional diagram of the LSTM cell, highlighting the cell state and three gates namely the forget gate, input gate and output gate. Here, the forget gate  $a(t)$  controls how much of the previous cell state  $q(t-1)$  should be retained in the current cell state  $q(t)$ . Concurrently, the proportion of new information  $\tilde{q}(t)$  to be integrated into the current cell state  $q(t)$  is determined by the input gate  $j(t)$ , based on the current input  $f(t)$  and previous hidden state  $g(t-1)$ . Lastly, the output gate  $u(t)$  decides the next hidden state or the final output  $g(t)$  based on the updated cell state  $q(t)$ , which is the combination of the past information retained from the forget gate and the new information added by the input gate. The mathematical framework of LSTM cell is provided in Eq. (10)-(15) as follows:

$$a(t) = \sigma(w_f^a f(t) + w_g^a g(t-1) + b_a), \quad (10)$$

$$j(t) = \sigma(w_f^j f(t) + w_g^j g(t-1) + b_j), \quad (11)$$

$$\tilde{q}(t) = \tanh(w_f^{\tilde{q}} f(t) + w_g^{\tilde{q}} g(t-1) + b_{\tilde{q}}), \quad (12)$$

$$u(t) = \sigma(w_f^u f(t) + w_g^u g(t-1) + b_u), \quad (13)$$

$$q(t) = a(t)q(t-1) + j(t)\tilde{q}(t), \quad (14)$$

$$g(t) = u(t)\tanh(q(t)), \quad (15)$$

where,  $w$  and  $b$  denote the learnable weight matrices applied to the inputs and the bias term, respectively. The outputs of the corresponding gates are generated by applying respective activation functions  $\sigma$  (sigmoid) and  $\tanh$  (hyperbolic tangent) on weighted sum, allowing the model to effectively manage the flow of information.

QLSTM is the quantum variant of the classical LSTM architecture used in machine learning. A significant distinguishing feature of QLSTM is the integration of VQCs that replace the traditional gating mechanisms within the LSTM cell. Fig. 4 presents the functional diagram of the QLSTM cell used in this work, showcasing the incorporation of four VQCs.

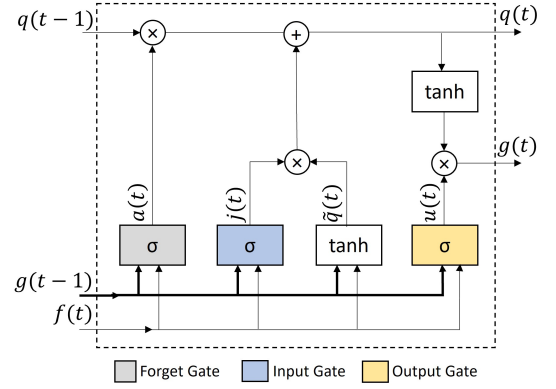


FIGURE 3. LSTM cell.

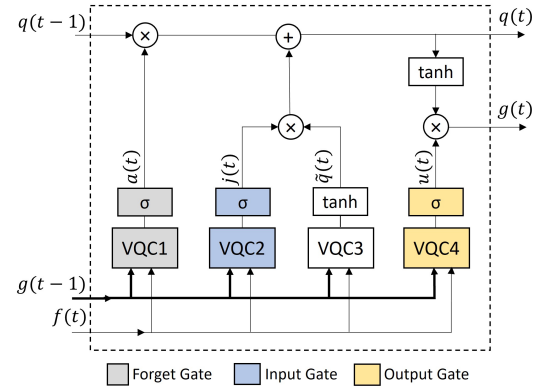


FIGURE 4. QLSTM cell.

The mathematical formulation of QLSTM cell is detailed in Eq. (16)-(21) as follows:

$$a(t) = \sigma(VQC_1(v_t)), \quad (16)$$

$$j(t) = \sigma(VQC_2(v_t)), \quad (17)$$

$$\tilde{q}(t) = \tanh(VQC_3(v_t)), \quad (18)$$

$$u(t) = \sigma(VQC_4(v_t)), \quad (19)$$

$$q(t) = a(t)q(t-1) + j(t)\tilde{q}(t), \quad (20)$$

$$g(t) = u(t)\tanh(q(t)), \quad (21)$$

where,  $v_t$  represents the current input  $f(t)$  and the previous hidden state  $g(t-1)$ . Similarly, the previous cell state, current cell state and the final output is represented by  $q(t-1)$ ,  $q(t)$  and  $g(t)$  respectively. The quantum circuits  $VQC1$  to  $VQC4$  refers to the homogenous VQCs that replace the classical LSTM gates (i.e. forget  $a(t)$ , input  $j(t)$ , update  $\tilde{q}(t)$ , and output  $u(t)$  gate). These quantum circuits transform the input and hidden state using quantum computations, potentially leading to more powerful and efficient sequence modelling. In this work, we used a 4 qubit VQC architecture as shown in Fig. 5, which is primarily based on three layers namely, the data encoding layer, variational layer and the measurement layer.

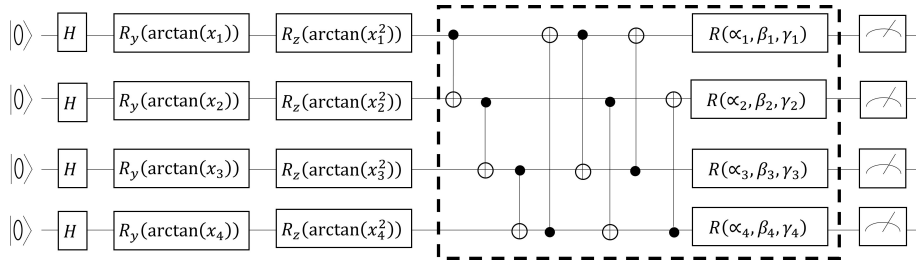


FIGURE 5. Architecture of VQC.

In the data encoding layer of the VQC, each qubit is initialised into an initial state  $|0\rangle$  and transformed into an unbiased superposition state having an equal probability of 0.5 using the hadamard gate. In addition, two rotation gates  $R_y(\theta_{1,i})$  and  $R_z(\theta_{2,i})$  are applied with angles dependant on the classical data. In these,  $\theta_{1,i} = \arctan(x_i)$  and  $\theta_{2,i} = \arctan(x_i^2)$  are calculated using the classical data samples  $x_i$  for each  $i^{th}$  wire considering  $i \in \{1, 2, 3, 4\}$ .

The variational layer introduces the entanglement using CNOT gates and parameterised rotations using rotation gate  $R(\alpha_i, \beta_i, \gamma_i) = R_x(\alpha_i)R_y(\beta_i)R_z(\gamma_i)$  along  $x$ ,  $y$  and  $z$  axis on the  $i^{th}$  wire. In this rotation,  $\alpha_i$ ,  $\beta_i$ , and  $\gamma_i$  are optimised during training to improve the performance of the model. Finally, the measurement layer collapses the quantum state of the qubits into classical data. For this, each qubit is measured along the  $z$  axis using the expectation value of the Pauli-Z gate output and this expectation value can be computed as  $|p_0^m|^2 - |p_1^m|^2$  to generate classical data. Here,  $|p_s^m|^2$  for  $s \in \{0, 1\}$  is the probability of a qubit being in state  $|s\rangle$  in the measurement layer. The classical data output after measurement is from +1, equivalent to  $|0\rangle$ , to -1, equivalent to  $|1\rangle$ , and values in between are representations of the superposition states. This output is considered the final output of the VQC which is further processed by a combination of the classical layers for the respective task such as prediction or classification.

## VI. MODEL TRAINING AND TESTING

This section presents details about data preparation, model training, parameters tuning and testing of the proposed forecasting model. The workflow of model training and testing with key components is shown in Fig. 6. In this study, the dataset used for experimentation is sourced from Belfast city council and is publicly accessible [36]. The input feature (a sequence) is created using historical information of the preceding three hours of the target pollutant's concentration. Alongside, VMD based features are created using a lag of the target pollutant being predicted, with experiments conducted to determine the optimum IMF number, denoted as  $K$  for each pollutant. The dataset is further divided into training, validation, and testing sets with a corresponding split ratio of 70%, 20%, and 10%. The indices in each split are progressively increased to maintain the integrity of the time series data. This method ensures that shuffling is avoided,

thereby preserving the temporal structure which is crucial for accurate forecasting. After splitting, the dataset is normalized using a z-score approach which is defined as follows:

$$x_{norm} = \frac{x - \mu}{v}, \quad (22)$$

where  $\mu$  and  $v$  are the corresponding mean and standard deviation of data  $x$ . Here, data is referred to both features and target data of the proposed model.

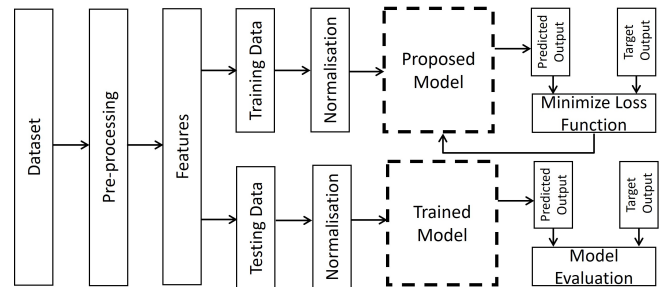


FIGURE 6. Workflow of model training and testing.

### A. MODEL PARAMETERS AND TUNING

In this work, we proposed AirVCQnet model with a learning network in which we considered two ConvID layers followed by a Max-Pooling and a QLSTM layer as shown in Fig. 1. Each layer required a careful selection of the parameters. In case of the ConvID layer, kernel size and number of filters or features at the output of the layer are key parameters. Considering the Max-Pooling layer which can reduce feature map using down sampling depending on the given kernel size value. The final layer of QLSTM captures the time dependencies based on the selection of a total number of hidden units or cells in the layer. In our proposed model, we have tuned the parameters like kernel size, out channels i.e., the number of filters of each ConvID layer and the number of hidden units of the QLSTM layer. We kept the kernel size of the Max-Pooling layer to a constant value of 2, this value is chosen after several experimental trials. We have also considered the learning rate as a tuning parameter to improve the forecasting model performance. We used the Optuna framework to find optimum tunable parameters of the proposed model by minimising the validation loss during training using AdaGrad optimiser [42], [43]. In the optimisation process, the number

of the hidden units in QLSTM layer is in the range [8 64], the kernel size and the out channel (also referred to as a number of output features) of each CNN layers are in the range of [2 5] and [4 32], respectively. In addition, the learning rate is used as an optimisable parameter within the range [ $1e^{-5}$   $1e^{-1}$ ] and applied early stopping criteria to manage overfitting and reduce training time. We used PennyLane software package with a maximum of 1000 epochs and trained the model on a high performance computing node equipped with a dual processor (2.5 GHz and L3 128 MB), 32 cores and, a maximum available RAM of 512 GB. Table. 2 provides a summary of the optimum values of the tunable parameters for each pollutant. Here, the optimum value of the  $K$  is found using numerous experimental trials with the objective to enhance the forecasting model performance for the respective pollutant.

**TABLE 2.** Optimised hyperparameters of the proposed model for all the pollutants.

Parameters	PM2.5	NO <sub>2</sub>	O <sub>3</sub>	PM10	SO <sub>2</sub>
Hidden units	12	55	46	35	59
Kernel size_1	2	3	5	2	5
Kernel size_2	5	4	5	4	5
Out channel_1	8	32	24	16	12
Out channel_2	30	16	19	4	15
Learning rate	$3.1e^{-3}$	$1.3e^{-3}$	$9.7e^{-3}$	$1.3e^{-2}$	$1.3e^{-3}$
K	5	3	2	4	2

### B. PERFORMANCE METRICS

The effectiveness of the proposed model is assessed using three widely used evaluation metrics namely  $R^2$ , RMSE, and MAE. Their mathematical formulation is provided in Eq. (23), (24) and (25) as follows:

$$R^2 = 1 - \frac{\sum_{i=1}^N (o_i - \hat{o}_i)^2}{\sum_{i=1}^N (o_i - \bar{o})^2}, \quad (23)$$

$$MAE = \frac{1}{N} \sum_{i=1}^N |o_i - \hat{o}_i|, \quad (24)$$

$$RMSE = \sqrt{\frac{1}{N} \sum_{i=1}^N (o_i - \hat{o}_i)^2}, \quad (25)$$

where  $o_i$ ,  $\bar{o}$ ,  $\hat{o}_i$ , and  $N$  represents the target output at the  $i^{th}$  sample, mean derived from target output, predicted output at the  $i^{th}$  sample, and total number of test samples, respectively. Both RMSE and MAE serve as crucial evaluation metrics and provide insight into the prediction accuracy of the forecasting model by reflecting the degree to which predicted output aligns with actual target values. Alongside these,  $R^2$ , also known as the coefficient of determination is another key metric indicating the extent to which the model captures the underlying data pattern, with a higher score indicating the

better fit between the actual and predicted output. Briefly, a forecasting model with low RMSE and MAE, coupled with  $R^2$  score closer to unity is considered to have strong predictive capability. This comprehensive evaluation informs researchers about the model's accuracy and enables them to enhance its predictive performance.

## VII. RESULTS AND DISCUSSION

This section presents and discusses the experimental findings of our proposed AirVCQnet model for all the aforementioned pollutants. The efficacy of the single-step forecasting model is assessed using key evaluation metrics such as RMSE, MAE and  $R^2$ . The results of the proposed AirVCQnet model for the prediction of PM2.5 level indicate 84% accuracy over test data along with corresponding RMSE and MAE values of 1.81 and 1.36, respectively. The forecasting model prediction performance for PM2.5 over test data is shown in Fig. 7. As can be seen, the proposed model closely fits the observed values. Our proposed model demonstrated its best performance by achieving  $R^2$  score of 92% and 91% for NO<sub>2</sub> and O<sub>3</sub> respectively, outperforming its prediction accuracy for the other pollutants. Furthermore, the model attained RMSE values of 4.84 and 5.34, along with MAE values of 3.86 and 4.04, respectively. For PM10 and SO<sub>2</sub> prediction, the proposed model achieved  $R^2$  score of 81% and 80%, respectively. Additionally, the model recorded RMSE of 3.31 and 0.5, along with MAE of 2.34 and 0.34 values, respectively. Overall, our proposed model achieved prediction accuracy within the range of 80% to 92% across the evaluated pollutants for 5 different time series. To better visualize the prediction performance of our proposed model in contrast to its classical counterpart, the prediction curves for NO<sub>2</sub>, O<sub>3</sub>, PM10, and SO<sub>2</sub> over the testing data as shown in Fig. 8, 9, 10, and 11, respectively.

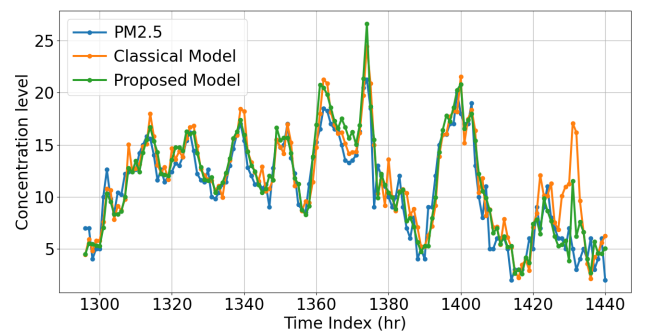


**FIGURE 7.** Comparison between actual and predicted data of PM2.5 over test data.

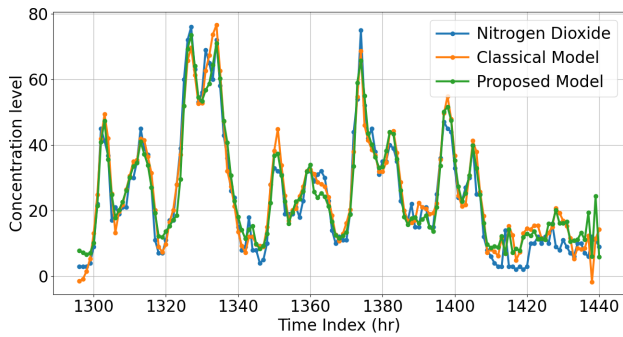


FIGURE 8. Comparison between actual and predicted data of NO<sub>2</sub> over test data.

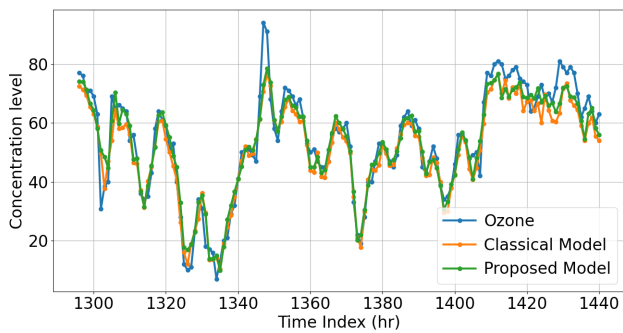


FIGURE 9. Comparison between actual and predicted data of O<sub>3</sub> over test data.

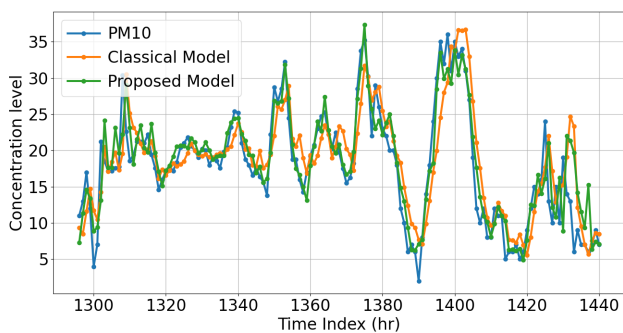


FIGURE 10. Comparison between actual and predicted data of PM10 over test data.

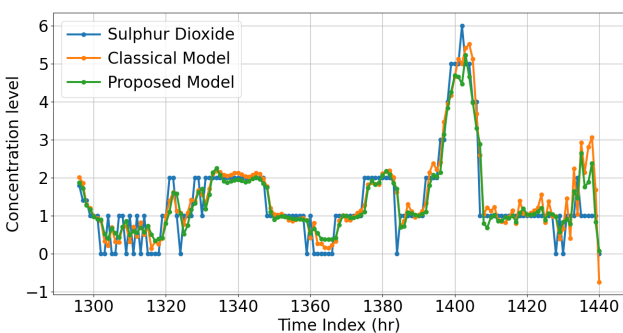


FIGURE 11. Comparison between actual and predicted data of SO<sub>2</sub> over test data.

To check the effectiveness of our proposed AirVCQnet model, a comparative analysis is performed with its classical counterpart using the same dataset and hyperparameters. The forecasting models' prediction performance is evaluated using the same assessment indicators. The results indicate that for PM<sub>2.5</sub>, PM<sub>10</sub> and SO<sub>2</sub> prediction, the classical model achieved a prediction accuracy of around 70% or higher with respect to R<sup>2</sup> score. The R<sup>2</sup>, RMSE and MAE values recorded for PM<sub>2.5</sub>, PM<sub>10</sub> and SO<sub>2</sub> is 70%, 69%, and 76%, 2.47, 4.25, and 0.55, 1.69, 3.19, and 0.38, correspondingly. Among all pollutants, O<sub>3</sub> and NO<sub>2</sub> stand out with prediction accuracies around or exceeding 90%. For O<sub>3</sub>, the R<sup>2</sup> score achieved is 89% with the corresponding RMSE and MAE values of 6.04 and 4.61. Notably, NO<sub>2</sub> is the only case, where the R<sup>2</sup> and MAE value of a classical model is comparable to the proposed model, with an R<sup>2</sup> score of 92% and MAE value of 3.85. On the other hand, the error score in terms of RMSE is reported as 5, which is slightly higher than the proposed model. Table. 3 highlights the performance improvement of the proposed model in terms of prediction accuracy based on R<sup>2</sup> score for all pollutants considered. Our findings revealed that our proposed model significantly improves the prediction performance with a gain of 14% for PM<sub>2.5</sub>, 2% for O<sub>3</sub>, 12% for PM<sub>10</sub>, and 4% for SO<sub>2</sub>. This is further supported by a reduction in error in terms of both RMSE and MAE within the range of 0.05 to 0.94 and 0.04 to 0.85 respectively. However, the performance of both models remained comparable for NO<sub>2</sub>, with AirVCQnet offering a modest improvement in the error reduction, as indicated by the RMSE value. Fig. 12, 13, and 14, summarised the performance comparison of the proposed model with the classical counterpart (i.e. VMD-CNN-LSTM) in terms of R<sup>2</sup> score, RMSE, and MAE values, respectively. The results of our comparative analysis clearly indicate that our proposed AirVCQnet outperformed its classical counterpart yielding a higher R<sup>2</sup> score and lower errors in terms of both RMSE and MAE across the evaluated pollutants.

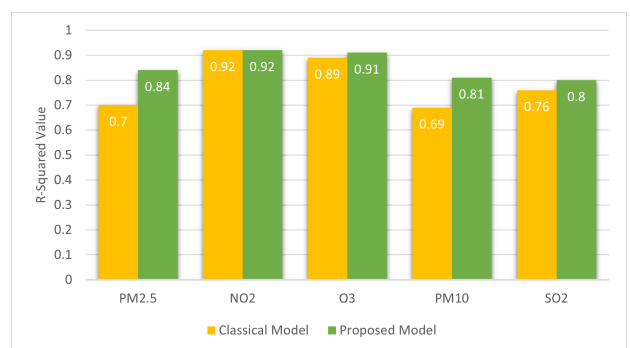


FIGURE 12. Comparison of models in terms of R<sup>2</sup>.

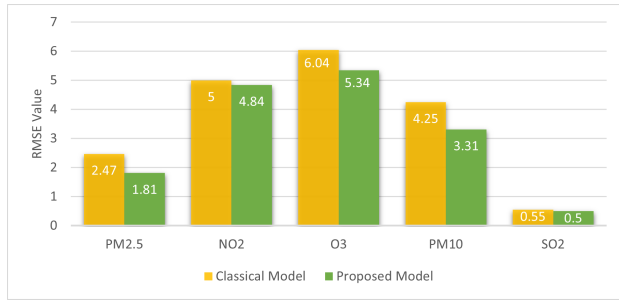


FIGURE 13. Comparison of models in terms of RMSE.

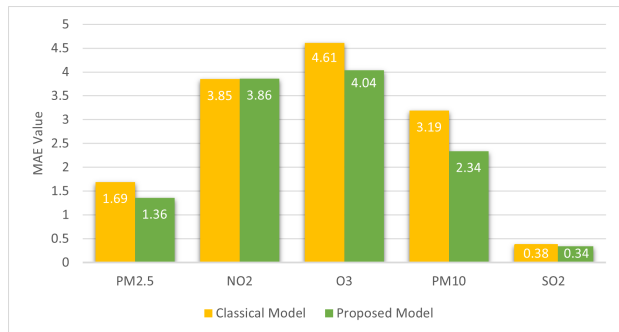


FIGURE 14. Comparison of models in terms of MAE.

TABLE 3. Performance comparison based on proposed model w.r.t R<sup>2</sup>.

Models	PM2.5	NO <sub>2</sub>	O <sub>3</sub>	PM10	SO <sub>2</sub>
Classical Model	0.70	0.92	0.89	0.69	0.76
Proposed Model	0.84	0.92	0.91	0.81	0.80
Gain	14	-	2	12	4

### VIII. CONCLUSION

Quantum machine learning offers significant computational advantages and plays a vital role in understanding and learning from complex datasets to build healthier, safer and better environments. Looking ahead, healthy ageing is one of the fundamental pillars of building healthier modern societies, with air quality standing out as one of the most critical influencing factors shaping this outcome. In this work, we investigated a hybrid forecasting model for five key air pollutants (i.e., PM<sub>2.5</sub>, NO<sub>2</sub>, O<sub>3</sub>, PM<sub>10</sub>, and SO<sub>2</sub>) using the emerging concept of quantum machine learning. Our proposed model takes advantage of features generated by VMD and CNN, which are further used to capture time dependencies using a QLSTM network. We investigated a four qubit VQC in QLSTM and found optimum proposed model parameters, including hyperparameters, to achieve a maximum R<sup>2</sup> score of 92%. Our findings revealed the superiority of the proposed model with the performance gain of 14% and reduced error when comparing its performance with its equivalent classical counterpart model with the same features and parameters. We anticipate that quantum inspired forecasting models can play

a crucial role in developing more accurate prediction systems that influence our future choices and policies’ of tomorrow.

### ACKNOWLEDGEMENTS

The work of Muhammad Fahim, Tuan-Vu Cao was supported in part by UKRI and European Commission under MISO Project, “Autonomous Multi-Format In-Situ Observation Platform for Atmospheric Carbon Dioxide and Methane Monitoring in Permafrost and Wetlands.” The work of Ruth Hunter was supported by the SPACE (Supportive Environments for Physical and Social Activity for Cognitive Health) Project (<https://www.qub.ac.uk/sites/space/>) funded by the ESRC Healthy Ageing Challenge under Grant ES/V016075/1. The work of T. Q. Duong was supported in part by the Canada Excellence Research Chair (CERC) Program CERC-2022-00109. All data supporting this study is provided as supplementary information accompanying this paper.

### REFERENCES

- [1] WHO, “WHO global air quality guidelines: particulate matter (PM<sub>2.5</sub> and PM<sub>10</sub>), ozone, nitrogen dioxide, sulfur dioxide and carbon monoxide,” accessed: Nov. 13, 2024. [Online]. Available: <https://www.who.int/publications/i/item/9789240034228>
- [2] WHO., “Ambient (outdoor) air pollution,” accessed: Nov. 13, 2024. [Online]. Available: [https://www.who.int/news-room/fact-sheets/detail/ambient-\(outdoor\)-air-quality-and-health](https://www.who.int/news-room/fact-sheets/detail/ambient-(outdoor)-air-quality-and-health)
- [3] G. Livingston, J. Huntley, K. Y. Liu, S. G. Costafreda, G. Selbæk, S. Alladi, D. Ames, S. Banerjee, A. Burns, C. Brayne, N. C. Fox, C. P. Ferri, L. N. Gitlin, R. Howard, H. C. Kales, M. Kivimäki, E. B. Larson, N. Nakasujja, K. Rockwood, Q. Samus, K. Shirai, A. Singh-Manoux, L. S. Schneider, S. Walsh, Y. Yao, A. Sommerlad, and N. Mukadam, “Dementia prevention, intervention, and care: 2024 report of the Lancet standing Commission,” *The Lancet*, vol. 404, pp. 572–628, 8 2024.
- [4] UN, “United Nations Sustainable Development Goals,” accessed: Nov. 13, 2024. [Online]. Available: <https://www.un.org/sustainabledevelopment/sustainable-development-goals>
- [5] WHO, “Air quality and health,” accessed: Nov. 13, 2024. [Online]. Available: <https://www.who.int/teams/environment-climate-change-and-health/air-quality-and-health/policy-progress/sustainable-development-goals-air-pollution>
- [6] DEFRA, “Clean Air Strategy,” accessed: Nov. 13, 2024. [Online]. Available: <https://www.gov.uk/government/publications/clean-air-strategy-2019>
- [7] HM, “25 year environment plan,” accessed: Nov. 13, 2024. [Online]. Available: <https://www.gov.uk/government/publications/25-year-environment-plan>
- [8] N. Keating, “A research framework for the United Nations Decade of Healthy Ageing (2021–2030),” *European Journal of Ageing*, vol. 19, no. 3, pp. 775–787, 2022.
- [9] X. Yu, L. Zheng, W. Jiang, and D. Zhang, “Exposure to air pollution and cognitive impairment risk: a meta-analysis of longitudinal cohort studies with dose-response analysis,” *Journal of Global Health*, vol. 10, 2020.
- [10] R. Peters, N. Ee, J. Peters, A. Booth, I. S. Mudway, and K. J. Anstey, “Air Pollution and Dementia: A Systematic Review,” *Journal of Alzheimer’s Disease*, vol. 70, pp. S145 – S163, 2019.
- [11] H. Chen, J. C. Kwong, R. Copes, P. Hystad, A. van Donkelaar, K. Tu, J. R. Brook, M. S. Goldberg, R. V. Martin, B. J. Murray, A. S. Wilton, A. Kopp, and R. T. Burnett, “Exposure to ambient air pollution and the incidence of dementia: A population-based cohort study,” *Environment International*, vol. 108, pp. 271–277, 2017.
- [12] M. Trott, C. L. Cleland, S. Akaraci, J. S. Valson, N. O’Kane, F. Kee, B. McGuinness, and R. F. Hunter, “Urban environment exposures and cognitive health: an evidence gap map of systematic reviews,” *Cities and Health*, 2024.

- [13] S. Jo, Y.-J. Kim, K. W. Park, Y. S. Hwang, S. H. Lee, B. J. Kim, and S. J. Chung, "Association of NO<sub>2</sub> and Other Air Pollution Exposures With the Risk of Parkinson Disease," *JAMA Neurology*, vol. 78, no. 7, pp. 800–808, 2021.
- [14] C. Duran-Aniotz, I. Moreno-Gonzalez, N. Gamez, N. Perez-Urrutia, L. Vegas-Gomez, C. Soto, and R. Morales, "Amyloid pathology arrangements in Alzheimer's disease brains modulate in vivo seeding capability," *Acta Neuropathologica Communications*, vol. 9, 2021.
- [15] S. Glover, C. Hill, B. McGuinness, A. J. McKnight, and R. F. Hunter, "Exploring the epigenome to identify biological links between the urban environment and neurodegenerative disease: an evidence review," *Cities and Health*, 2024.
- [16] UKRI, "Healthy Ageing," accessed: Nov. 13, 2024. [Online]. Available: <https://www.ukri.org/what-we-do/browse-our-areas-of-investment-and-support/healthy-ageing>
- [17] W. Zheng and J. Hu, "Multivariate Time Series Prediction Based on Temporal Change Information Learning Method," *IEEE Transactions on Neural Networks and Learning Systems*, vol. 34, no. 10, pp. 7034–7048, 2023.
- [18] J. Borah, S. Kumar, N. Kumar, M. S. M. Nadzir, M. G. Cayetano, H. Ghayvat, S. Majumdar, and N. Kumar, "AiCareBreath: IoT-Enabled Location-Invariant Novel Unified Model for Predicting Air Pollutants to Avoid Related Respiratory Disease," *IEEE Internet of Things Journal*, vol. 11, no. 8, pp. 14 625–14 633, 2024.
- [19] T. H. Putri, R. E. Caraka, T. Toharudin, Y. Kim, R.-C. Chen, P. U. Gio, A. D. Sakti, R. S. Pontoh, I. R. Pratiwi, F. A. L. Nugraha, T. S. Azzahra, J. J. Cereia, G. Darmawan, D. Y. Faidah, and B. Pardamean, "Fine-Tuning of Predictive Models CNN-LSTM and CONV-LSTM for Nowcasting PM<sub>2.5</sub> Level," *IEEE Access*, vol. 12, pp. 28 988–29 003, 2024.
- [20] P. Dey, S. Dev, and B. S. Phelan, "CombineDeepNet: A Deep Network for Multistep Prediction of Near-Surface PM<sub>2.5</sub> Concentration," *IEEE Journal of Selected Topics in Applied Earth Observations and Remote Sensing*, vol. 17, pp. 788–807, 2024.
- [21] L. Wang, X. Jin, Z. Huang, H. Zhu, Z. Chen, Y. Liu, and H. Feng, "Short-Term PM<sub>2.5</sub> Prediction Based on Multi-Modal Meteorological Data for Consumer-Grade Meteorological Electronic Systems," *IEEE Transactions on Consumer Electronics*, vol. 70, no. 1, pp. 3464–3474, 2024.
- [22] W. Ren, D. Ma, and M. Han, "Multivariate Time Series Predictor With Parameter Optimization and Feature Selection Based on Modified Binary Salp Swarm Algorithm," *IEEE Transactions on Industrial Informatics*, vol. 19, no. 4, pp. 6150–6159, 2023.
- [23] X. Wang, J. Yan, X. Wang, and Y. Wang, "Air Quality Forecasting Using the GRU Model Based on Multiple Sensors Nodes," *IEEE Sensors Letters*, vol. 7, no. 7, pp. 1–4, 2023.
- [24] X. Ouyang, Y. Yang, W. Zhou, Y. Zhang, H. Wang, and W. Huang, "City-Trans: Domain-Adversarial Training With Knowledge Transfer for Spatio-Temporal Prediction Across Cities," *IEEE Transactions on Knowledge and Data Engineering*, vol. 36, no. 1, pp. 62–76, 2024.
- [25] Y. Y. Hong and J. B. D. Santos, "Day-Ahead Spatiotemporal Wind Speed Forecasting Based on a Hybrid Model of Quantum and Residual Long Short-Term Memory Optimized by Particle Swarm Algorithm," *IEEE Systems Journal*, vol. 17, no. 4, pp. 6081–6092, 2023.
- [26] Z. Qu, X. Liu, and M. Zheng, "Temporal-Spatial Quantum Graph Convolutional Neural Network Based on Schrödinger Approach for Traffic Congestion Prediction," *IEEE Transactions on Intelligent Transportation Systems*, vol. 24, pp. 8677–8686, 8 2023.
- [27] W. Yu, L. Yin, C. Zhang, Y. Chen, and A. X. Liu, "Application of Quantum Recurrent Neural Network in Low Resource Language Text Classification," *IEEE Transactions on Quantum Engineering*, 2024.
- [28] M. Grossi, N. Ibrahim, V. Radescu, R. Loredo, K. Voigt, C. von Altrock, and A. Rudnik, "Mixed Quantum-Classical Method for Fraud Detection With Quantum Feature Selection," *IEEE Transactions on Quantum Engineering*, vol. 3, pp. 1–12, 2022.
- [29] J. A. Ansere, E. Gyamfi, V. Sharma, H. Shin, O. A. Dobre, and T. Q. Duong, "Quantum Deep Reinforcement Learning for Dynamic Resource Allocation in Mobile Edge Computing-based IoT Systems," *IEEE Transactions on Wireless Communications*, pp. 1–1, 2023.
- [30] K. Phalak and S. Ghosh, "Shot Optimization in Quantum Machine Learning Architectures to Accelerate Training," *IEEE Access*, vol. 11, pp. 41 514–41 523, 2023.
- [31] Y. Yu, G. Hu, C. Liu, J. Xiong, and Z. Wu, "Prediction of Solar Irradiance One Hour Ahead Based on Quantum Long Short-Term Memory Network," *IEEE Transactions on Quantum Engineering*, vol. 4, pp. 1–15, 2023.
- [32] Y.-Y. Hong, C. J. E. Arce, and T.-W. Huang, "A Robust Hybrid Classical and Quantum Model for Short-Term Wind Speed Forecasting," *IEEE Access*, vol. 11, pp. 90 811–90 824, 2023.
- [33] Y. Y. Hong, C. L. P. P. Rioflorida, and W. Zhang, "Hybrid deep learning and quantum-inspired neural network for day-ahead spatiotemporal wind speed forecasting," *Expert Systems with Applications*, vol. 241, 5 2024.
- [34] A. Ceschini, A. Rosato, and M. Panella, "Hybrid Quantum-Classical Recurrent Neural Networks for Time Series Prediction," in *2022 International Joint Conference on Neural Networks (IJCNN)*, 2022, pp. 1–8.
- [35] Y. Cao, X. Zhou, X. Fei, H. Zhao, W. Liu, and J. Zhao, "Linear-layer-enhanced quantum Long Short-Term Memory for carbon price forecasting," *Quantum Machine Intelligence*, vol. 5, 12 2023.
- [36] N. I. Air, "Download air quality data - Northern Ireland," accessed: Dec. 1, 2022. [Online]. Available: <https://www.airqualityni.co.uk/data>
- [37] K. Dragomiretskiy and D. Zosso, "Variational Mode Decomposition," *IEEE Transactions on Signal Processing*, vol. 62, no. 3, pp. 531–544, 2014.
- [38] F. Naz, M. Fahim, A. A. Cheema, N. T. Viet, T.-V. Cao, R. Hunter, and T. Q. Duong, "Two-Stage Feature Engineering to Predict Air Pollutants in Urban Areas," *IEEE Access*, vol. 12, pp. 114 073–114 085, 2024.
- [39] C. Nguyen, T. M. Hoang, and A. A. Cheema, "Channel Estimation Using CNN-LSTM in RIS-NOMA Assisted 6G Network," *IEEE Transactions on Machine Learning in Communications and Networking*, vol. 1, pp. 43–60, 2023.
- [40] Y. Tang, L. Zhang, F. Min, and J. He, "Multiscale Deep Feature Learning for Human Activity Recognition Using Wearable Sensors," *IEEE Transactions on Industrial Electronics*, vol. 70, no. 2, pp. 2106–2116, 2023.
- [41] S. Hochreiter and J. Schmidhuber, "Long Short-Term Memory," *Neural Computation*, vol. 9, pp. 1735–1780, 11 1997.
- [42] T. Akiba, S. Sano, T. Yanase, T. Ohta, and M. Koyama, "Optuna: A Next-generation Hyperparameter Optimization Framework," in *Proceedings of the 25th ACM SIGKDD International Conference on Knowledge Discovery and Data Mining*, 2019.
- [43] J. Duchi, E. Hazan, and Y. Singer, "Adaptive Subgradient Methods for Online Learning and Stochastic Optimization," *Journal of Machine Learning Research*, vol. 12, no. 61, pp. 2121–2159, 2011.



FAREENA NAZ received her B.S. degree in computer science from The University of Agriculture, Pakistan, in 2008, and the M.S. degree in computer science from COMSATS University, Islamabad, Pakistan, in 2010. She is currently a Ph.D. student at the Queen's University Belfast, UK, and part of the EU SPACE project. Her research interests include quantum machine learning, data analytics, air pollution modelling, and natural language processing.



MUHAMMAD FAHIM received his B.S. with distinction from Gomal University, Pakistan in 2007. He got M.S. from the National University of Computer and Emerging Sciences (NUCES), Pakistan in 2009. He got his Ph.D. degree from Kyung Hee University, South Korea in February 2014. He worked as Post-Doctoral Fellow at the Department of Computer Engineering, Kyung Hee University, South Korea. He served as an Assistant Professor in the Department of Computer and Software Engineering, Faculty of Engineering and Natural Sciences, Istanbul Sabahattin Zaim University, Istanbul, Turkey for 3 years. He also led the Machine Learning research laboratory in Istanbul Sabahattin Zaim University. He worked as an Assistant Professor at the Institute of Information Systems, Innopolis University, Innopolis, Russia for four years. Currently, he is lecturer in School of Electronics, Electrical Engineering and Computer Science, Queen's University Belfast, UK. His research interests include machine learning models, wearable computing, digital signal processing, and behaviour recognition in intelligent environments.



**ADNAN AHMAD CHEEMA** (Senior Member, IEEE) received the B.Sc. degree from the COMSATS University, Pakistan., M.Sc. degree from the King's College London, U.K., and the Ph.D. degree from the Durham University, U.K., in 2006, 2008 and 2015, respectively. From 2015 to 2017, he was a postdoctoral Research Associate at Durham University. Since 2017, he is working as a Lecturer in electronics engineering at Ulster University, U.K. He is a Senior Member of URSI and secured a research grant portfolio exceeding £4.5 million. He played a key role in founding the Advanced Wireless Technologies Lab (AWTL) at Ulster University and currently leads AWTL. His current research interests include quantum machine learning, channel estimation and modelling, mmWave/THz communications and RF sensing.



**RUTH HUNTER** is a Professor of Public Health and Planetary Health at the Centre for Public Health, Queen's University Belfast, and Director of the WHO Collaborating Centre for research and training in systems thinking and complexity science for NCD prevention and control. Her work primarily involves investigating how we can improve where we live (i.e. our built, social and natural environments) for better population health and planetary health. She is particularly interested in research at the intersection of public health and planetary health. She is the principal investigator of the ESRC funded SPACE project (grant reference ES/V016075/1).



**BRADLEY D. E. MCNIVEN** received his PhD degree in condensed matter physics from Memorial University in 2024. He is currently a postdoctoral research fellow at Memorial University with a focus on quantum algorithm development and quantum information science. His current research interests include quantum machine learning and optimization, experimental quantum information, laser spectroscopy, and quantum matter.



**TRUNG Q. DUONG** (Fellow) is a Canada Excellence Research Chair (CERC) and a Full Professor at Memorial University, Canada. He is also an adjunct professor at Queen's University Belfast, UK, a visiting professor at Kyung Hee University, South Korea, and an adjunct professor at Duy Tan University, Vietnam. His current research interests include wireless communications, quantum machine learning, and quantum optimization. His current research interests include wireless communications, quantum machine learning, and quantum optimisation.

Dr. Duong has served as an Editor/Guest Editor for the IEEE Transactions on Wireless Communications, IEEE Transactions on Communications, IEEE Transactions on Vehicular Technology, IEEE Communications Letters, IEEE Wireless Communications Letters, IEEE Wireless Communications, IEEE Communications Magazines, and IEEE Journal on Selected Areas in Communications. He received the Best Paper Award at the IEEE VTC-Spring 2013, IEEE ICC 2014, IEEE GLOBECOM 2016, 2019, 2022, IEEE DSP 2017, IWCMC 2019, 2023, 2024 and IEEE CAMAD 2023, 2024. He is the Editor in Chief of IEEE Communications Surveys & Tutorials and an IEEE ComSoc Distinguished Lecturer. He has received the two prestigious awards from the Royal Academy of Engineering (RAEng): RAEng Research Chair and the RAEng Research Fellow. He is the recipient of the prestigious Newton Prize 2017. He is a Fellow of the Engineering Institute of Canada (EIC), the Canadian Academy of Engineering (CAE), the Institution of Engineering and Technology (IET), and Asia-Pacific Artificial Intelligence Association (AAIA).



**TUAN-VU CAO** is a senior scientist at NILU Norwegian Institute for Air Research. He received PhD in electrical engineering from University of Oslo in 2012. He has a long experience in both academic and industry. From 2012 to 2018, he worked as Adjunct Associate Professor at University of Tromsø (Norway), a postdoctoral fellow at Norwegian University of Science and Technology and senior engineers at WINS Instrumentation AS and Prediktor AS for various projects such as

monitoring nutrient food content; wireless DST real time instrumentation; micropower sensor interface in nanometer CMOS Technology. He joined NILU from 2018. His research areas and interests are Enabling technologies and Autonomous Systems for Environmental monitoring and management. He is the PI of Horizon Europe project- MISO (2023-2026) – Autonomous Multi-Format In-Situ Observation Platform for Atmospheric Carbon Dioxide and Methane Monitoring in Permafrost & Wetlands; WP leader of NFR IKTPLUSS project AirQMan (2021-2025) - Low Latency Air Quality Management; co-PI of EEA grant project– HAPADS (2020-2023)-a novel air mobile monitoring system enables end-users to make information-driven decisions to mitigate air pollution exposure; key designer and technical coordinator for NFR 273394-“Leopard-Wearable particle detector enabling safer working environments” (2018-2020).

...